Photoinduced Electron Transfer in Tetrathiafulvalene–Porphyrin–Fullerene Molecular Triads

by **Paul A. Liddell**, **Gerdenis Kodis**, **Linda de la Garza**, **Jeffrey L. Bahr**, **Ana L. Moore***, **Thomas A. Moore***, and **Devens Gust***

Department of Chemistry and Biochemistry, Center for the Study of Early Events in Photosynthesis, Arizona State University, Tempe, AZ 85287, USA

Dedicated to Professor *André M. Braun* on the occasion of his 60th birthday

The two molecular triads **1a** and **1b** consisting of a porphyrin (P) covalently linked to a fullerene (C_{60}) electron acceptor and tetrathiafulvalene (TTF) electron-donor moiety were synthesized, and their photochemical properties were determined by transient absorption and emission techniques. Excitation of the free-base-porphyrin moiety of the TTF–P_{2H}–C_{60} triad **1a** in tetrahydro-2-methylfuran solution yields the porphyrin first excited singlet state TTF–$^1P_{2H}$–C_{60}, which undergoes photoinduced electron transfer with a time constant of 25 ps to give TTF–$P_{2H}^{\bullet+}$–$C_{60}^{\bullet-}$. This intermediate charge-separated state has a lifetime of 230 ps, decaying mainly by a charge-shift reaction to yield a final state, $TTF^{\bullet+}$–P_{2H}–$C_{60}^{\bullet-}$. The final state has a lifetime of 660 ns, is formed with an overall yield of 92%, and preserves *ca.* 1.0 eV of the 1.9 eV inherent in the porphyrin excited state. Similar behavior is observed for the zinc analog **1b**. The TTF-$P_{Zn}^{\bullet+}$–$C_{60}^{\bullet-}$ state is formed by ultrafast electron transfer from the porphyrinatozinc excited singlet state with a time constant of 1.5 ps. The final $TTF^{\bullet+}$–P_{Zn}–$C_{60}^{\bullet-}$ state is generated with a yield of 16%, and also has a lifetime of 660 ns. Although charge recombination to yield a triplet has been observed in related donor-acceptor systems, the $TTF^{\bullet+}$–P–$C_{60}^{\bullet-}$ states recombine to the ground state, because the molecule lacks low-energy triplet states. This structural feature leads to a longer lifetime for the final charge-separated state, during which the stored energy could be harvested for solar-energy conversion or molecular optoelectronic applications.

Introduction. – Photosynthetic-energy conversion is characterized by efficient light absorption followed by photoinduced electron transfer to generate long-lived, highly energetic charge-separated states. The potential energy of these states is ultimately used to produce biologically useful energy in forms such as proton motive force, adenosine triphosphate (ATP), and reduction potential. A great deal of progress has been made in mimicry of the photosynthetic process by means of artificial molecular constructs based on porphyrins or related chlorophyll analogs [1–10]. Artificial photosynthetic reaction centers have been married to synthetic antenna arrays [11], and inserted into the membranes of liposomes, where they harvest light energy to drive the production of proton motive force and ATP [1][12][13].

In recent years, we have extensively investigated carotenoid (C) porphyrin (P) fullerene (C_{60}) triad molecules as mimics for photosynthetic reaction centers [14–21]. Excitation of the porphyrin moiety of these molecules yields the first excited singlet state C–^{1}P–C_{60}, which undergoes photoinduced electron transfer to give C–$P^{\bullet+}$–$C_{60}^{\bullet-}$. Electron transfer from the carotenoid competes with charge recombination, forming a final $C^{\bullet+}$–P–$C_{60}^{\bullet-}$ state. With suitable molecular architectures, this state is generated with quantum yields of essentially unity. Under most conditions, charge recombination of $C^{\bullet+}$–P–$C_{60}^{\bullet-}$ yields the carotenoid triplet state, ^{3}C–P–C_{60}, rather than the ground state. Although this recombination process leads to interesting

spin effects [15] and forms the basis of a magnetically controlled molecular logic gate [19], it also limits the lifetime of the charge separation. This is potentially undesirable for applications in the areas of solar-energy conversion or molecular-scale optoelectronics where the energy stored in the charge-separated state must be coupled to other chemical or electronic processes.

Recombination of $C^{\bullet+}-P-C_{60}^{\bullet-}$ to yield the carotenoid triplet is possible because the energy of the triplet is very low – significantly below that of the charge-separated state. Thus, we have sought other electron donors with higher-lying triplet states where such recombination could not occur. Tetrathiafulvalene (=2-(1,3-dithiol-2-ylidene)-1,3-dithiole; TTF) derivatives are well-known donor species in intermolecular charge-transfer systems, and have recently been paired with fullerenes to produce donor-acceptor dyads with interesting properties [22–34]. In addition, suitably substituted TTF derivatives have nearly identical first and second oxidation potentials, making them good candidates for charge accumulation systems. For these reasons, we synthesized tetrathiafulvalene-porphyrin-fullerene triads **1a** and **1b** and related model compounds (*Fig. 1*), and investigated their photochemical properties by time-resolved spectroscopic techniques.

Results. – *Synthesis.* The synthesis began with porphyrin diester **3** (*Fig. 1*). Acid-catalyzed hydrolysis gave **4**, which was converted to aldehyde **5** *via* reduction of the ester to the alcohol, which was then oxidized with manganese dioxide. Base-catalyzed hydrolysis of the remaining ester moiety yielded **6**, whose COOH group was next protected as the 3,5-dimethylbenzyl ester ($\rightarrow$ **7**). Reaction [35] of **7**, C_{60}, and sarcosine gave porphyrin-fullerene dyad **8**. Such reactions are known to produce only a single isomer, an adduct to a double bond at a 6,6-ring fusion in C_{60}. The protecting group was removed from **8** by BBr_3, and the resulting acid **9** was coupled with tetrathiafulvalene-4-methanol to give free-base triad **1a** in 80% yield. Stirring **1a** with zinc acetate in CH_2Cl_2 yielded zinc triad **1b** quantitatively.

The triads were characterized by NMR and mass spectrometry. The various model compounds used in this study were prepared by similar methods, and details are given in the *Exper. Part*. The synthesis of porphyrin-fullerene dyad **11a** has been reported previously [36].

Cyclic Voltammetry. Electrochemical measurements were undertaken to investigate the redox properties of TTF model **10** and the triads **1a** and **1b**. These were needed to estimate the energies of charge-separated states. The measurements were carried out with a *Pine Instrument Co*. potentiostat (model *AFRDE4*) at room temperature with a glassy-carbon working electrode, a Ag/Ag^+ reference electrode, and a Pt-wire counter electrode. Measurements were performed in benzonitrile containing 0.1M tetrabutylammonium hexafluorophosphate, and ferrocene as an internal redox standard (oxidation at 0.46 V *vs.* SCE). Compound **10** featured reversible oxidation waves at 0.43 and 0.87 V *vs.* SCE. These values are similar to those reported for TTF derivatives with related structures [37]. Free-base triad **1a** showed reversible oxidations at 0.42, 0.83, and 1.07 V *vs.* SCE, and reductions at -0.60, -0.99, and -1.19 V. The first two oxidations are ascribed to the TTF moiety, and the third to the oxidation of the porphyrin ring. The first two reduction waves are due to the fullerene moiety, and the third to the free-base porphyrin [38]. Zinc-containing triad **1b** demonstrated oxidations

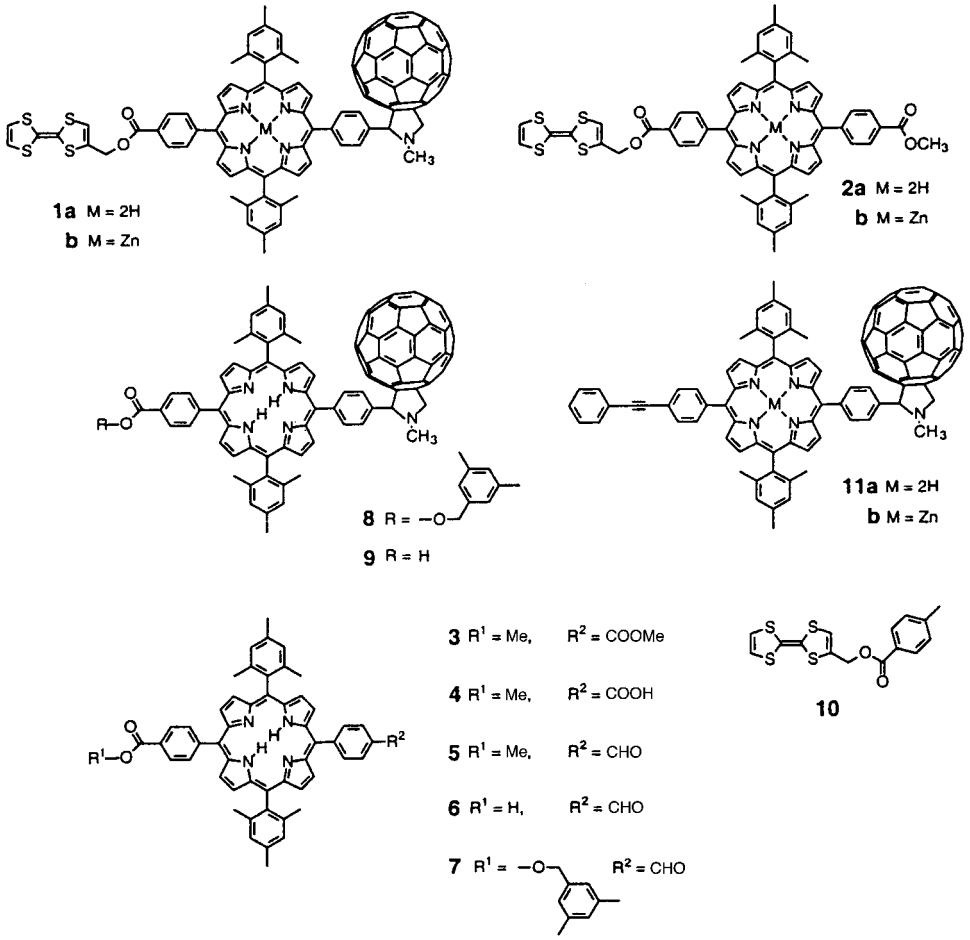

Fig. 1. *Structures of the triads, model compounds, and precursors*

at 0.42, 0.83, and 1.23 V *vs.* SCE, and reductions at −0.58 and −0.99 V. The first oxidation is due to the TTF moiety, whereas the second is a two-electron process, corresponding to the second oxidation of the TTF moiety and the first oxidation of the porphyrinatozinc. The reductions are again ascribed to the fullerene. These potentials are all very similar to those measured for model porphyrins and fullerenes, indicating that linking the moieties in the triad does little to perturb the individual redox centers.

Absorption Spectra. The absorption spectrum of free-base triad **1a** in tetrahydro-2-methylfuran is shown in *Fig. 2*, *a*. The maxima are at *ca*. 255, 305, 368 (sh), 415, 482, 514, 548, 591, 648, and 705 (very weak) nm. Similarly, the absorption spectrum of zinc triad **1b** (*Fig. 2*, *b*) shows maxima at *ca*. 255, 305, 405 (sh), 420, 518, 557, 598, and 705 (very weak) nm. The absorption maximum in both compounds at 305 nm is ascribed to the tetrathiafulvalene moiety, as demonstrated by the absorption spectrum of model TTF compound **10**, which has bands at 305 and 365 nm and a very weak, broad absorption at

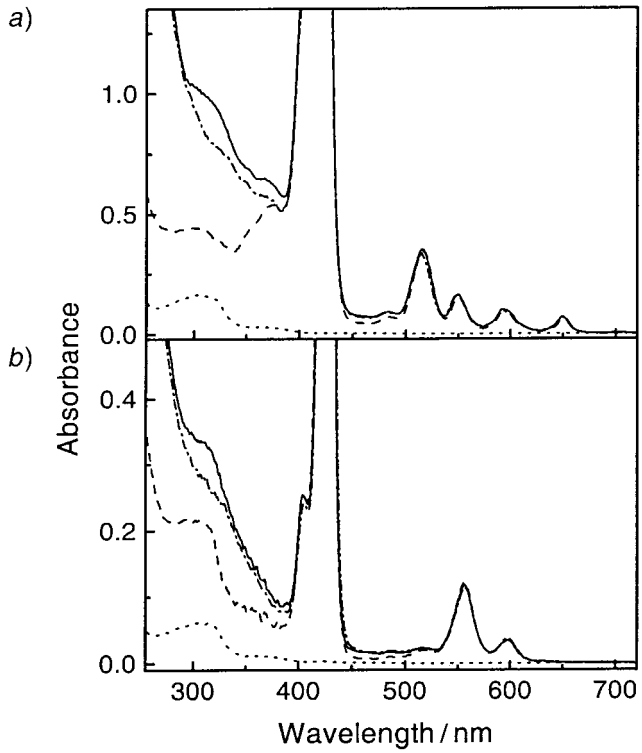

Fig. 2. *Absorption spectra in tetrahydro-2-methylfuran of* a) *TTF–P_{2H}–C_{60} triad* **1a** (—), *TTF–P_{2H} dyad* **2a** (– – –), *P_{2H}–C_{60} dyad* **11a** (–•–•–), *and TTF model compound* **10** (• • •). The spectra for the porphyrin-containing moieties are normalized at the long-wavelength Q-band absorption at 658 nm. b) *TTF–P_{Zn}–C_{60} triad* **1b** (—), *TTF–P_{Zn} dyad* **2b** (– – –), *P_{Zn}–C_{60} dyad* **11b** (–•–•–), *and TTF model compound* **10** (• • •). The spectra for the porphyrin-containing moieties are normalized at the long-wavelength Q-band absorption at 598 nm.

ca. 450 nm. In both triads, the bands at *ca*. 255 and 705 nm, with continuous weak absorption at intermediate wavelengths, are characteristic of the fullerene. The remaining major bands in the spectra may be assigned to the porphyrin moieties, by reference to spectra of model porphyrins such as **3**.

For comparison, *Fig. 2* also shows the spectra of model compounds **2a**, **2b**, **11a**, and **11b** normalized at either 648 nm (free-base porphyrins) or 598 nm (porphyrinatozinc complexes). Absorption maxima for model dyad **11a** are found at 305, 368 (sh), 415, 482, 514, 548, 591, and 648 nm. Similarly, the absorption spectrum of model dyad **11b** shows maxima at 305, 405 (sh), 420, 518, 557, and 598 nm. Subtraction of the absorption spectrum of **2a** from **1a**, or **2b** from **1b**, yields a spectrum characteristic of a fullerene with a substitution pattern similar to that of the fullerene moiety of **1a**. Subtraction of the spectrum of **11a** from that of **1a** or **11b** from **1b**, gives the spectrum of a TTF derivative such as **10**. In fact, the absorption spectra of the triads are essentially linear combinations of the spectra of the TTF, porphyrin, and fullerene chromophores, and show no significant perturbations indicative of strong interactions between the linked

moieties. The analysis of the absorption spectra of **1a** and appropriate models shows that with excitation at 650 nm, it is possible to excite the free-base porphyrin almost exclusively. Similarly, excitation of **1b** at 600 nm will produce almost exclusively the porphyrinatozinc first excited singlet state.

Fluorescence-Emission Spectra. The fluorescence-emission spectra for **1a** and **2a** in tetrahydro-2-methylfuran, obtained with equal absorbance at the excitation wavelength of 590 nm, are shown in *Fig. 3,a*. The emission for the TTF-P_{2H}–C_{60} triad is quenched by a factor of 260, relative to the emission of the TTF-P_{2H} dyad. Quenching is also seen for the zinc triad, whose emission in tetrahydro-2-methylfuran is shown in *Fig. 3,b*. The emission of **1b** is characteristic of porphyrinatozinc, with maxima at 603 and 654 nm. However, it is weaker than that of model dyad **2b** by a factor of 650. By analogy with various porphyrin–fullerene dyads reported in the literature, we ascribe this quenching to photoinduced electron transfer from the porphyrin to the fullerene. As shown below, this assumption is verified by additional spectroscopic studies.

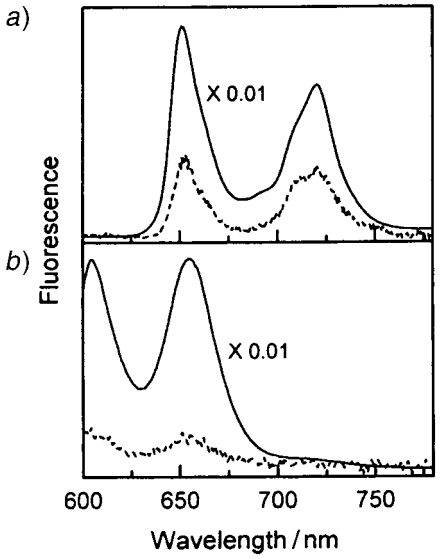

Fig. 3. *Corrected fluorescence-emission spectra obtained in tetrahydro-2-methylfuran solution with excitation at 590 nm:* a) *TTF–P_{2H} dyad* **2a** (—) *and TTF–P_{2H}–C_{60} triad* **1a** (– – –). The samples have the same absorbance at 590 nm, and the emission spectrum of **2a** is multiplied by 0.01 to facilitate comparison. b) *TTF–P_{Zn} dyad* **2b** (—) *and TTF–P_{Zn}–C_{60} triad* **1b** (– – –). The samples have the same absorbance at 590 nm, and the emission spectrum of **2b** is multiplied by 0.01 to facilitate comparison.

Time-Resolved Fluorescence. The very strong quenching observed for **1a** and **1b** allows the possibility that the steady-state fluorescence emission that is observed in these compounds may be due to very minor, but strongly fluorescent impurities, rather than the triads themselves. Thus, we turned to time-resolved fluorescence techniques to obtain more accurate data. *Fig. 4* shows typical fluorescence decays obtained by the single-photon timing technique, and determined in tetrahydro-2-methylfuran solution with excitation at 590 nm and detection at 650 nm, where both free-base and porphyrinatozinc moieties emit.

As illustrated in *Fig. 4*, the fluorescence decay of TTF-free-base porphyrin dyad **2a** could be fitted as a single-exponential process with a lifetime of 6.5 ns ($\chi^2 = 1.09$). This lifetime indicates a slight quenching of the 11.0-ns lifetime typical for porphyrins of this general type [36]. The quenching is ascribed to photoinduced electron transfer from

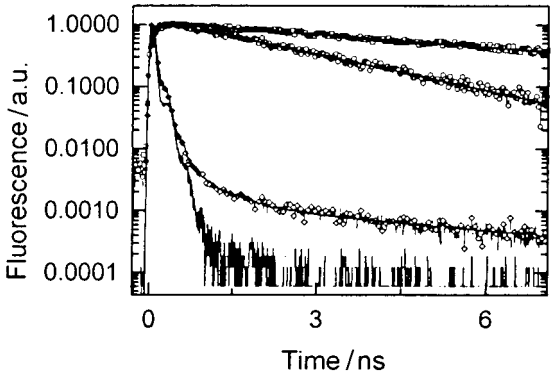

Fig. 4. *Fluorescence decays in tetrahydro-2-methylfuran solution with excitation at 590 nm and detection at 650 nm: THF–P_{2H}–C_{60} triad* **1a** (◇)), *TTF–P_{2H} dyad* **2a** (□), *TTF–P_{Zn} dyad* **2b** (○), *and instrument response function* (—). The solid lines through the data points for the three compounds are the best theoretical fits to the data and yield the time constants reported in the text. Note the log scale for fluorescence intensity.

the TTF moiety to form a $TTF^{\bullet+}-P_{2H}{}^{\bullet-}$ charge-separated state. The decay from TTF–P_{2H}–C_{60} triad **1a** was fitted as three exponential decays with lifetimes of 29 ps, 177 ps, and 3.5 ns ($\chi^2 = 1.25$). The latter two components made up $\leq 5\%$ of the total amplitude, and are ascribed to minor impurities or fitting artifacts. The 29-ps component is ascribed to strong quenching of the porphyrin first excited singlet state by the fullerene, which is consistent with the steady-state results reported above.

The fluorescence decay of TTF-P_{Zn} dyad **2b** was fitted as a single-exponential process with a time constant of 2.2 ns ($\chi^2 = 1.18$). This lifetime is similar to that of model porphyrinatozinc complexes of this general type, and indicates no significant quenching of the porphyrin first excited singlet state by the TTF moiety. With TTF–P_{Zn}–C_{60} triad **1b**, no significant fluorescence emission was observed. This suggests that the lifetime of the porphyrinatozinc first excited singlet state is shorter than the time resolution of the spectrometer (*ca.* 5 ps).

Time-Resolved Absorption. Transient absorption experiments were undertaken to better quantify the interconversions of the various excited states in these compounds and to allow detection of nonemissive states such as charge-separated species. Solutions (*ca.* $1 \cdot 10^{-3}$ M) in tetrahydro-2-methylfuran were excited with *ca.* 100 fs laser pulses, and the transient absorption spectra were recorded by means of the pump-probe method. Excitation was at 650 and/or 600 nm. Spectra were recorded in the 930–1070 nm and 450–760 nm regions, at times ranging from −50 to 4500 ps relative to the laser flash. Data were fitted globally by means of singular value decomposition methods [39][40].

Free-Base-Porphyrin Systems. It was postulated above that quenching of the first excited singlet state of the free-base porphyrin of triad **1a** was due to photoinduced electron transfer to the fullerene. Support for this conclusion comes from a previously reported spectroscopic investigation of porphyrin–fullerene dyad **11a** [36]. This dyad, rather than dyad **8**, was chosen as a model for **1a** because the solubility of **8** was not high enough to obtain an acceptable signal-to-noise ratio. The sample was excited at 650 nm, where most of the light is absorbed by the porphyrin. Immediately after excitation,

absorptions characteristic of $^1P_{2H}-C_{60}$ were observed. The singlet evolved into the $P_{2H}^{\bullet+}-C_{60}^{\bullet-}$ charge-separated state with a time constant of 25 ps. This state was readily identified by the fullerene radical anion absorption in the 1000 nm region and by the very broad porphyrin radical cation absorption in the VIS region. The charge-separated state decayed to the ground state with a lifetime of 3.0 ns. Transient-absorption studies at several wavelengths showed that excitation of the porphyrin moiety does not lead to significant population of the fullerene first excited singlet state by singlet-singlet energy transfer; photoinduced electron transfer is the only important decay pathway for $^1P_{2H}-C_{60}$ [36].

Fig. 5,a shows results obtained from excitation of triad **1a** in tetrahydro-2-methylfuran solution with a 600-nm laser pulse. This light is absorbed mainly by the porphyrin moiety, generating TTF-$^1P_{2H}-C_{60}$. Over time, a new transient species grew in with an absorbance maximum at *ca.* 1000 nm (inset in *Fig. 5,a*). This is ascribed to the fullerene radical anion. When the spectrum was monitored at 1000 nm, the radical anion absorption grew in with a time constant of 25 ps, which corresponds, within experimental error, to the decay time for the porphyrin first excited singlet state, as determined by the time-resolved fluorescence studies (29 ps), and to the rise time of $P_{2H}^{\bullet+}-C_{60}^{\bullet-}$ in dyad **11a** (25 ps). The fullerene radical anion absorption band did not

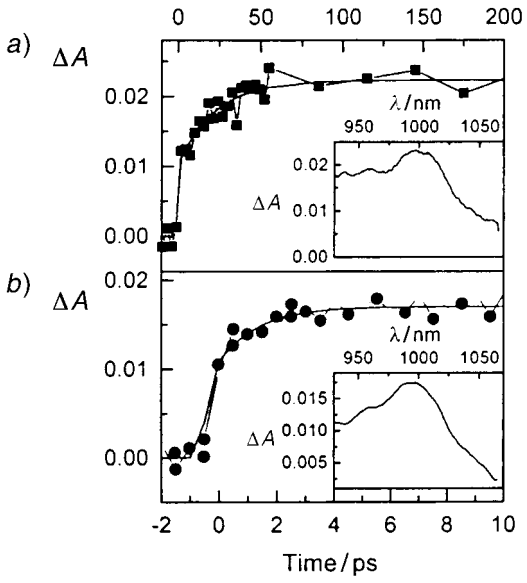

Fig. 5. a) *Transient absorption at 1000 nm of a tetrahydro-2-methylfuran solution of TTF–P_{2H}–C_{60} triad* **1a** *following excitation at 600 nm with a* ca. *100-fs laser pulse.* The data, measured in the 1000-nm region, show the rise of the fullerene radical anion of the TTF–$P_{2H}^{\bullet+}-C_{60}^{\bullet-}$ charge-separated state, with a time constant of 25 ps (fit shown as a solid line). The inset shows the spectrum 2 ns after excitation: the anion transient absorption does not decay on this time scale. b) *Transient absorption at 1000 nm of a tetrahydro-2-methylfuran solution of TTF–P_{Zn}–C_{60} triad* **1b** *following excitation at 600 nm with a* ca. *100-fs laser pulse.* The data, measured in the 1000-nm region, show the rise of the fullerene radical anion of the TTF–$P_{Zn}^{\bullet+}-C_{60}^{\bullet-}$ charge-separated state, with a time constant of 1.5 ps (fit shown as a solid line). The inset shows the spectrum 2 ns after excitation; the anion transient absorption does not decay on this time scale.

decay over a period of 4 ns, which is the longest time scale available on the spectrometer.

Fig. 6,a shows decay-associated spectra for triad **1a**, determined by global analysis of transient absorption data obtained with excitation at 650 nm. The best theoretical fit to the data set was achieved with three components: 25 ps, 230 ps, and a component that did not decay on this time scale. The 25-ps component has bleaching bands at 515, 550, 590, and 650 nm, and negative amplitude in the red part of the spectrum, corresponding to stimulated emission bands at 650 and 720 nm. These are all characteristic of the free-base porphyrin, and are assigned to decay of the porphyrin first excited singlet state and concomitant formation of the porphyrin radical cation with characteristic absorption in 600–800 nm region. This result is indicative of formation of the $TTF-P_{2H}^{\bullet+}-C_{60}^{\bullet-}$ charge-separated state by photoinduced electron transfer.

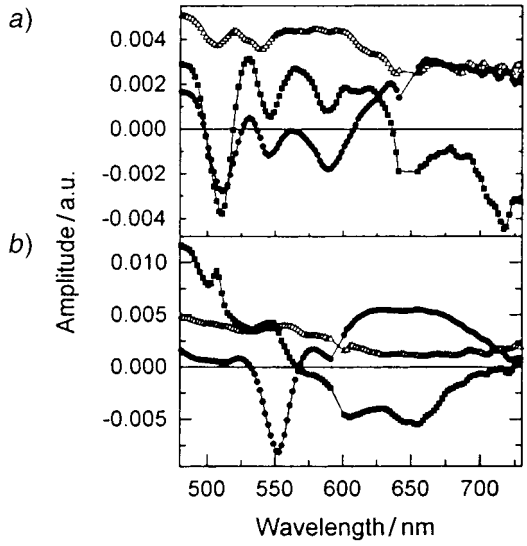

Fig. 6. a) *Decay-associated spectra for free-base triad* **1a**, *determined by global analysis of transient absorption data obtained with excitation of a tetrahydro-2-methylfuran solution at 650 nm*. Two components have time constants of 25 ps (■) and 230 ps (●), and the third is non-decaying on this time scale (△). b) *Decay-associated spectra for zinc triad* **1b**, *determined by global analysis of transient absorption data obtained with excitation of a tetrahydro-2-methylfuran solution at 600 nm*. Two components have time constants of 1.5 ps (■) and 570 ps (●), and the third is non-decaying on this time scale (△).

The 230-ps component is mostly of positive amplitude, but has almost the same bleaching bands at the 25-ps component. It is most interesting that this component has negative amplitude at the maxima of 515, 550, and 590 nm bleaching bands. Negative amplitude in this case indicates the disappearance of these bands and the rise of a new transient species that does not have bleaching bands at these wavelengths. We ascribe the 230-ps component to decay of $TTF-P_{2H}^{\bullet+}-C_{60}^{\bullet-}$ by charge shift from the TTF moiety, leading to formation of a $TTF^{\bullet+}-P_{2H}-C_{60}^{\bullet-}$ charge-separated state. The spectrum of the nondecaying component is consistent with the tetrathiafulvalene radical cation, with absorption maxima at *ca*. 430, 520, and 580 nm [22].

Porphyrinatozinc Systems. Zinc dyad **11b** in tetrahydro-2-methylfuran was also investigated by the pump-probe technique with excitation at 600 nm, where most of the absorption is by the porphyrinatozinc. As with analog **11a**, excitation produced the porphyrin first excited singlet state $^1P_{Zn}-C_{60}$, but this state rapidly decayed by photoinduced electron transfer to yield $P_{Zn}^{\bullet+}-C_{60}^{\bullet-}$. *Fig. 7,a* shows the rise of the transient absorption of the fullerene radical anion at 1000 nm. The data are best fit with an exponential process having a time constant of 1.5 ps. *Fig. 7,b* illustrates the decay of $P_{Zn}^{\bullet+}-C_{60}^{\bullet-}$, monitored at the same wavelength. The lifetime is 680 ps.

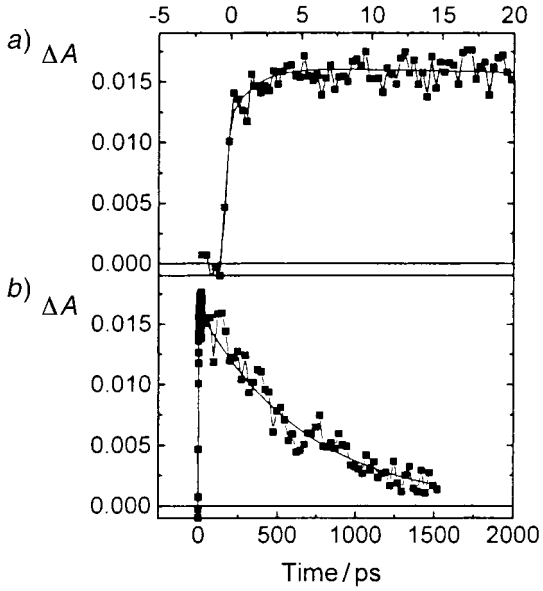

Fig. 7. a) *Rise and* b) *decay of the transient absorption at 1000 nm due to the fullerene radical anion of the* $P_{Zn}^{\bullet+}-C_{60}^{\bullet-}$ *charge-separated state, generated by photoinduced electron transfer after excitation of dyad* **11b** *in tetrahydro-2-methylfuran with a 600 nm*, ca. *100-fs laser pulse.* The excitation light is absorbed mainly by the zinc porphyrin moiety. The solid lines correspond to theoretical fits to the data as exponential processes with time constants of 1.5 ps (rise in *a*)) and 680 ps (decay in *b*)).

Turning now to triad **1b**, similar transient absorption experiments with excitation at 600 nm showed that the laser flash yielded $TTF-{}^1P_{Zn}-C_{60}$, which decayed to give the $TTF-P_{Zn}^{\bullet+}-C_{60}^{\bullet-}$ charge-separated state with a time constant of 1.5 ps (*Fig. 5,b*). The fullerene radical anion absorption in the 1000-nm region is readily apparent in the inset in *Fig. 5,b*. The radical anion absorption did not decay on the time scale of the measurement. Decay-associated spectra for **1b** are shown in *Fig. 6,b*, and feature components with lifetimes of 1.5 ps and 570 ps, plus a component that does not decay on this time scale.

The 1.5-ps component has bands at 515, 560, 600, and 650 nm that are characteristic of the porphyrinatozinc. The negative amplitude in the longer-wavelength portion of the spectrum (stimulated emission bands at 600 and 650 nm) and the positive amplitude in the shorter-wavelength portion of the spectrum are indicative of the decay of the porphyrin first excited singlet state and the concomitant formation of the porphyr-

inatozinc radical cation. These results confirm the formation of the $TTF-P_{Zn}^{\bullet+}-C_{60}^{\bullet-}$ charge-separated state. Charge separation is very fast, and comparable with the solvation time of the porphyrin excited singlet state. For this reason, the porphyrin bleaching bands at 515 and 560 nm appear initially as positive, blue-shifted bands that move to the red during their formation.

The 570-ps component is mostly of positive amplitude on the longer-wavelength side of the spectrum and has bleaching bands at shorter wavelengths. This component has a negative amplitude at the maximum of the 560-nm bleaching band, indicating a rise of transient absorption that does not show bleaching at that wavelength. This indicates decay of $TTF-P_{Zn}^{\bullet+}-C_{60}^{\bullet-}$ and concomitant formation of the $TTF^{\bullet+}-P_{Zn}-C_{60}^{\bullet-}$ charge-separated state by a charge-shift reaction. The long-lived component that does not decay on this time scale has a spectrum consistent with the tetrathiafulvalene radical cation and fullerene radical anion, as expected for the final $TTF^{\bullet+}-P_{Zn}-C_{60}^{\bullet-}$ species.

Lifetime of the Charge-Separated State. The lifetimes of the final charge-separated states in triads **1a** and **1b** are too long to be measured by the pump-probe technique, and appear as non-decaying spectral components in *Figs. 5* and *6*. We turned to nanosecond flash photolysis to determine their decay properties. A deoxygenated sample of **1a** in tetrahydro-2-methylfuran was excited wtih *ca*. 5-ns laser pulses at 600 nm, and the resulting spectral changes were measured. *Fig. 8* shows the decay of the fullerene radical anion absorption measured at 1000 nm and the TTF radical cation absorption at 580 nm. The data at both wavelengths were fitted satisfactorily with a single-exponential decay with a time constant of 660 ns. Similar experiments with zinc triad **1b** yielded the same time constant. Thus, $TTF^{\bullet+}-P_{2H}-C_{60}^{\bullet-}$ and $TTF^{\bullet+}-P_{Zn}-C_{60}^{\bullet-}$ have identical lifetimes. The decay product was the molecular ground state, as the decay of the charge-separated state was not accompanied by the concomitant rise of triplet states. Excitation of **1a** did produce a small amount of porphyrin triplet state, with characteristic maxima at *ca*. 450 and 780 nm. The appearance of these transients was prompt ($\leq$20 ns), and is most likely due to a small amount of intersystem crossing in **1a**, or in minor impurities. In the absence of oxygen, these minor transients did not

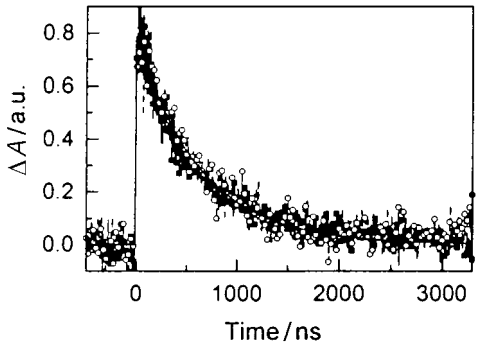

Fig. 8. *Decay of the fullerene radical anion absorption, measured at 1000 nm* (○) *and the TTF radical cation absorption at 580 nm* (■), *determined after excitation of a tetrahydro-2-methylfuran solution of free-base triad* **1a** *with a* ca. *5-ns laser pulse at 600 nm*. Also shown is an exponential fit to the data with a time constant of 660 ns (solid line).

decay in a 5-μs time window, but the decay rate was enhanced when air was admitted to the sample.

Discussion. – *Energetics.* The transient spectral data for **1a** and **1b** will be discussed in terms of the kinetic schemes shown in *Fig. 9*. The energies of the excited singlet states are estimated as the wavelength average of the longest-wavelength absorption and shortest-wavelength emission maxima of the triads and appropriate model compounds. The free-base porphyrin first excited singlet state lies 1.90 eV above the ground state, whereas the corresponding porphyrinatozinc excited state is at 2.06 eV. The fullerene first excited singlet state is at 1.75 eV, and previous results have shown that, in dyad **11a**, direct excitation of this state is followed by photoinduced electron transfer to yield $P^{\bullet+}-C_{60}^{\bullet-}$ [36]. However, in the experiments described here, the fullerene first excited singlet state was not significantly populated either by direct excitation or by energy transfer, and so it is not indicated in *Fig. 9*. Based on the electrochemical results described above, the energies of the $TTF-P_{2H}^{\bullet+}-C_{60}^{\bullet-}$, $TTF-P_{Zn}^{\bullet+}-C_{60}^{\bullet-}$, $TTF^{\bullet+}-P_{2H}-C_{60}^{\bullet-}$, $TTF^{\bullet+}-P_{Zn}-C_{60}^{\bullet-}$ and $TTF^{\bullet+}-P_{2H}^{\bullet-}-C_{60}$ charge-separated states

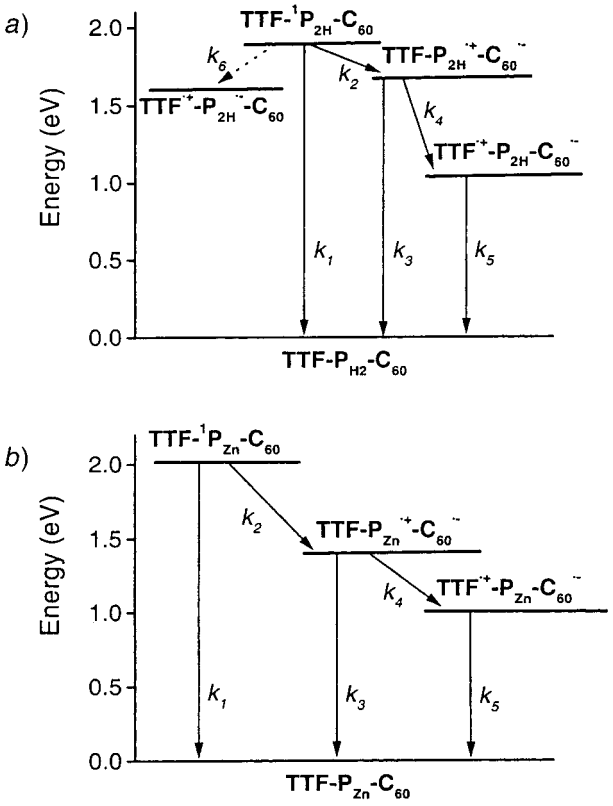

Fig. 9. *Relevant excited and transient states for* a) *triad* **1a** *and* b) *triad* **1b** *and interconversion pathways.* Each reaction step (*e.g.*, *Step 2*) is labeled with its corresponding rate constant (*e.g.*, k_2).

are estimated as 1.67, 1.41, 1.01, 1.01, and 1.61 eV, respectively. These estimates are not corrected for any coulombic effects that may be present.

Kinetics Processes: Free-Base Triad **1a**. The porphyrin first excited singlet state in **1a** can, of course, decay by the usual photophysical processes of intersystem crossing to the triplet, fluorescence, and internal conversion. The sum of the rate constants for these processes is shown as k_1 in *Fig. 9,a*, and may be estimated as $9.1 \cdot 10^7\ s^{-1}$, based on the 11.0-ns lifetime of model free-base porphyrins mentioned above. In principle, this state could also decay by singlet-singlet energy transfer to the fullerene, or by electron transfer from the TTF moiety, or to the fullerene. As mentioned above, singlet-singlet energy transfer was not observed. The TTF–^{1}P state in dyad **2a** has a lifetime of 6.5 ns, and is thus slightly quenched relative to model porphyrins. This quenching is attributed to photoinduced electron transfer from the TTF moiety to yield the TTF$^{\bullet+}$–P$_{2H}^{\bullet-}$ charge-separated state (analogous to *Step 6* in *Fig. 9,a*). From this model compound, the value of k_6 may be calculated by *Eqn. 1*, where τ_f is the observed lifetime of the excited singlet state (6.5 ns). Thus, k_6 is $6.3 \cdot 10^7\ s^{-1}$ (corresponding to a quantum yield of 0.41 in dyad **2a**).

$$1/\tau_f = k_1 + k_6 \tag{1}$$

The lifetime of TTF–^{1}P$_{2H}$–C$_{60}$ in triad **1a** is only 25 ps, indicating that by far the major pathway for decay of the porphyrin excited singlet state is photoinduced electron transfer to the fullerene to generate TTF–P$_{2H}^{\bullet+}$–C$_{60}^{\bullet-}$ (*Step 2* in *Fig. 9,a*). *Eqn. 2* yields a value for k_2 of $4.0 \cdot 10^{10}\ s^{-1}$, which in turn gives a quantum yield for the initial charge-separated state, Φ_{in}, equal to 1.0.

$$1/\tau_f = k_1 + k_2 + k_6 \tag{2}$$

The TTF–P$_{2H}^{\bullet+}$–C$_{60}^{\bullet-}$ species may either recombine to give the ground-state by *Step 3*, or evolve by electron transfer from the TTF moiety to the porphyrin radical cation to give the final TTF$^{\bullet+}$–P$_{2H}$–C$_{60}^{\bullet-}$ charge-separated state (*Step 4*). The reciprocal of the 230 ps time constant observed for the decay of TTF–P$_{2H}^{\bullet+}$–C$_{60}^{\bullet-}$ and rise of TTF$^{\bullet+}$–P$_{2H}$–C$_{60}^{\bullet-}$ is the sum of the rate constants for these processes, k_3 and k_4. A value of $3.3 \cdot 10^8\ s^{-1}$ for k_3 may be estimated from the 3.0-ns lifetime of the P$_{2H}^{\bullet+}$–C$_{60}^{\bullet-}$ state of dyad **11a**. Therefore, k_4 equals $4.0 \cdot 10^9\ s^{-1}$. The quantum yield of the final TTF$^{\bullet+}$–P$_{2H}$–C$_{60}^{\bullet-}$ charge-separated state, Φ_{fi}, is given by *Eqn. 3* and equals 0.92. The TTF$^{\bullet+}$–P$_{2H}$–C$_{60}^{\bullet-}$ state decays to the ground-state with a rate constant k_5 of $1.5 \cdot 10^6\ s^{-1}$, based on the 660-ns lifetime observed in the nanosecond transient absorption experiments.

$$\Phi_{fi} = \Phi_{in}\ (k_4/(k_3 + k_4)) \tag{3}$$

Kinetics Processes: Zinc Triad **1b**. The relevant states are shown in *Fig. 9,b*. A value for rate constant k_1 of $4.6 \cdot 10^8$ may be estimated from the 2.2-ns lifetime of TTF–^{1}P in dyad **2b**. As mentioned earlier, this lifetime is similar to that of porphyrinatozinc model compounds, and demonstrates that the porphyrinatozinc first excited singlet state is not quenched by electron transfer from the TTF moiety. It is not surprising that no

significant electron transfer is observed in this case, even though quenching was noted for free-base dyad **2a**. In the first place, the driving force for the process is much reduced in the zinc triad, because reduction potentials for porphyrinatozinc complexes are *ca.* 0.3 V more negative than those for the corresponding free base. In addition, the unperturbed excited state lifetime of the porphyrinatozinc is significantly shorter than that for the free base, limiting the effect of alternate decay pathways.

Given a value for k_1, the rate constant for photoinduced electron transfer, k_2, may be calculated from the 1.5-ps lifetime of TTF–^{1}P$_{Zn}$–C$_{60}$ that was determined from the pump-probe transient absorption measurements: $k_2 = (1/1.5 \cdot 10^{-12}\ s) - 4.6 \cdot 10^8\ s^{-1} = 6.7 \cdot 10^{11}\ s^{-1}$. The rate constant for decay of the initially-formed TTF–P$_{Zn}^{\bullet+}$–C$_{60}^{\bullet-}$ state, k_3, is taken as the reciprocal of the 680-ps lifetime of P$_{Zn}^{\bullet+}$–C$_{60}^{\bullet-}$ in dyad **11b**, or $1.5 \cdot 10^9\ s^{-1}$. The transient-absorption experiments for **1b** gave a time constant of 570 ps for formation of TTF$^{\bullet+}$–P$_{Zn}$–C$_{60}^{\bullet-}$ from TTF–P$_{Zn}^{\bullet+}$–C$_{60}^{\bullet-}$. Given these values, k_4, the rate constant for the charge-shift reaction in **1b**, is found to be $2.8 \cdot 10^8\ s^{-1}$. The quantum yield of TTF–P$_{Zn}^{\bullet+}$–C$_{60}^{\bullet-}$ based on light absorbed by the porphyrin is 1.0, whereas that of the final TTF$^{\bullet+}$–P$_{Zn}$–C$_{60}^{\bullet-}$ species is 0.16. The rate constant for decay of TTF$^{\bullet+}$–P$_{Zn}$–C$_{60}^{\bullet-}$ to the ground state, k_5, equals $1.5 \cdot 10^6\ s^{-1}$, as determined from the 660-ns lifetime of the state.

Conclusions. – It is interesting to contrast the properties of the free-base and zinc triads with one another, and with related triads. With free-base triad **1a**, photoinduced electron transfer to the fullerene dominates the other decay pathways and gives the TTF–P$_{2H}^{\bullet+}$–C$_{60}^{\bullet-}$ state with a yield of unity. This is the case even though the thermodynamic driving force for *Step 6*, which leads to TTF$^{\bullet+}$–P$_{2H}^{\bullet-}$–C$_{60}$, is greater than that for *Step 2* by 0.06 eV. These reactions occur in the normal region of the *Marcus* relationship [41][42], where increased driving force increases the electron-transfer rate. The larger rate constant for *Step 2* than for *Step 6* may be ascribed to stronger electronic coupling of the porphyrin and fullerene than of the porphyrin and the TTF moiety. At the simplest level, there are four bonds separating the π-electron systems of the TTF and the *meso*-positioned aryl substituent at the porphyrin moiety, but only three connecting the fullerene π-electron system and the aryl substituent. It is also likely that the low solvent and internal-reorganization energies (λ_s and λ_i) for electron transfer characteristic of the fullerene [14][16][20][21][43–46] move *Step 2* closer to the maximum of the *Marcus* relationship, where $-\Delta G^\circ = \lambda$, thereby increasing the rate. In the case of zinc-containing triad **1b**, the driving force for *Step 2* in *Fig. 9,b* is 0.42 eV larger than the driving force for the comparable step in free-base triad **1a**, leading to extremely rapid electron transfer.

The quantum yield of the initial charge-separated state in both triads is essentially unity. Thus, the yield of the final, long-lived charge-separated state is determined by the partitioning of the TTF–P$^{\bullet+}$–C$_{60}^{\bullet-}$ states between charge recombination to the ground-state (*Step 3*) and charge shift to the TTF to form the final TTF$^{\bullet+}$–P–C$_{60}^{\bullet-}$ species (*Step 4*). For free-base triad **1a**, the driving force for charge shift *Step 4* is a respectable 0.66 eV. The driving force for recombination of TTF–P$^{\bullet+}$–C$_{60}^{\bullet-}$ is so large, at 1.67 eV, that recombination is well into the *Marcus* inverted region where the higher driving force leads to smaller rate constants. The result of these two factors is a high overall yield of charge separation of 92%. With zinc triad **1b**, the driving force for

charge shift is reduced to 0.40 eV, causing that reaction to be slower than in **1a**. At the same time, the driving force for charge recombination, at 1.41 eV, is smaller than it is for **1a**, but since the reaction occurs in the inverted region, this implies a faster rate of charge recombination. These two factors work together to limit the yield of the final $TTF^{\bullet+}-P_{Zn}-C_{60}^{\bullet-}$ state to only 16%.

Recombination of the $TTF^{\bullet+}-P-C_{60}^{\bullet-}$ final charge-separated state in the free-base porphyrin or porphyrinatozinc could in principle be either a direct, single-step process, or a two-step sequence wherein a rate-determining, endergonic recombination to the $TTF-P^{\bullet+}-C_{60}^{\bullet-}$ state is followed by rapid recombination *via Step 3*. Charge recombination by such a two-step process has been previously observed in some triad molecules, whereas, in others, the one-step process or a mixture of the two mechanisms has been observed [14][20][47–49]. Although the free-energy difference between the $TTF^{\bullet+}-P_{2H}-C_{60}^{\bullet-}$ and $TTF-P_{2H}^{\bullet+}-C_{60}^{\bullet-}$ states is 0.26 eV larger than that between the $TTF^{\bullet+}-P_{Zn}-C_{60}^{\bullet-}$ and $TTF-P_{Zn}^{\bullet+}-C_{60}^{\bullet-}$ states, the final charge-separated states of **1a** and **1b** have identical lifetimes in tetrahydro-2-methylfuran of 660 ns. This indicates that charge recombination occurs directly to the ground-state (*Step 5* in *Fig. 9*), rather than *via* the two-step process.

As mentioned in the introduction, a significant number of fullerene-containing dyad and triad molecules that demonstrate photoinduced electron transfer also feature charge recombination to yield a triplet state rather than the ground state. This sort of recombination requires an energetically accessible triplet state and is favored by the low reorganization energy for electron transfer characteristic of fullerenes [20]. In the case of triads **1a** and **1b**, recombination to yield a triplet state is not observed, suggesting that the lowest-lying triplet states for all of the component chromophores are at significantly higher energy than the $TTF^{\bullet+}-P-C_{60}^{\bullet-}$ state in these molecules. Thus, the lifetime of the final state is enhanced, compared, for example, to carotenoid-containing triads of related structure and with similar energetics for electron transfer. Quantitative evaluation of this effect is not facile because of the differences in electronic coupling among the various molecular systems.

The TTF family of electron donors is potentially attractive for inclusion in multicomponent molecular devices such as **1a** and **1b**, not only for the reasons mentioned above, but also because some TTF derivatives have nearly identical first and second oxidation potentials. Fullerene derivatives can in principle function as readily reversible multiple-electron acceptors. Thus, the incorporation of both TTF and fullerene moieties in the same molecule allows the possibility of multiphoton, multielectron molecular switching applications. TTF-Containing molecules are currently of great interest due to various potential molecular (opto)electronic and sensing applications [30][33].

Experimental Part

General. The synthesis of **11a** has been previously reported [36]. ^{1}H-NMR Spectra: *Varian Unity* spectrometers at 300 or 500 MHz; unless otherwise specified, $CDCl_3$ solns. with $SiMe_4$ as internal reference; δ in ppm, J in Hz. MS: *Kratos-MS-50* mass spectrometer for high-resolution, at 8 eV in the FAB mode; matrix-assisted laser desorption/ionization time-of-flight spectrometer (MALDI-TOF) for other MS; m/z. UV/VIS ground-state absorption spectra: *Shimadzu UV2100U* UV-VIS spectrometer; λ_{max} in nm.

Steady-State Fluorescence-Emission Spectra. They were measured using a *SPEX Fluorolog-2* and corrected for variations in the response of the system with wavelength. Excitation was produced by a 450-W Xe lamp and

single-grating monochromator. Fluorescence was detected at 90° to the excitation beam *via* a single-grating monochromator and an *R928* photomultiplier tube having *S-20* spectral response operating in the single-photon counting mode.

Fluorescence-Decay Measurements. They were performed with *ca.* $1 \cdot 10^{-5}$ M solns. by the single-photon timing method. The excitation source was a cavity-dumped *Coherent-700* dye laser pumped by a frequency-doubled *Coherent-Antares* 76s Nd:YAG laser. Fluorescence emission was detected at the magic angle by a single-grating monochromator and microchannel plate photomultiplier (*Hamamatsu R2809U-11*). The instrument response time was *ca.* 35–50 ps, as verified by scattering from *Ludox AS-40*. The spectrometer was controlled by software based on a LabView program from *National Instruments* [50].

Nanosecond Transient-Absorption Measurements. They were made with excitation from an *Opotek* optical parametric oscillator pumped by the third harmonic of a *Continuum Surelight* Nd:YAG laser. The pulse width was *ca.* 5 ns, and the repetition rate was 10 Hz. The transient absorbance was measured by means of a diode detector equipped with 10-nm bandpass interference filters. The detection portion of the spectrometer has been described elsewhere [51].

Femtosecond Transient-Absorption Measurements. The apparatus consisted of a kHz-pulsed laser source and a pump-probe optical setup. The laser pulse train was provided by a Ti: Sapphire regenerative amplifier (*Clark-MXR*, model *CPA-1000*) pumped by a diode-pumped CW solid-state laser (*Spectra Physics*, model *Millennia V*). The typical laser pulse was 100 fs at 790 nm, with a pulse energy of 0.9 mJ at a repetition rate of 1 kHz. Most of the laser energy (80%) was used to pump an optical parametric amplifier (*IR-OPA*, *Clark-MXR*). The excitation pulse was sent through a computer-controlled optical-delay line. The remaining laser output (20%) was focused into a 1.2-cm rotating quartz plate to generate a white-light continuum. The continuum beam was further split into two identical parts and used as the probe and reference beams. The probe and reference signals were focused onto two separated optical-fiber bundles coupled to a spectrograph (*Acton Research*, model *SP275*). The spectra were acquired on a dual diode-array detector (*Princeton Instruments*, model *DPDA-1024*) [52].

Lifetimes. To determine the number of significant lifetime components in the transient absorption data, singular-value-decomposition analysis [39][40] was carried out with locally written software based on the MatLab 5.0 program (*MathWorks, Inc.*) Decay-associated spectra were then obtained by fitting the transient absorption change curves over a selected wavelength region simultaneously as described by *Eqn. 4*, where $\Delta A(\lambda,t)$ is the observed absorption change at a given wavelength at time delay t and n is the number of kinetic components used in the fitting. A plot of $A_i(\lambda)$ *vs.* wavelength, *i.e.*, a decay-associated spectrum, represents the amplitude spectrum of the i^{th} kinetic component, which has a lifetime of τ_i.

$$\Delta A(\lambda,t) = \sum_{i=1}^{n} A_i(\lambda) \exp(-t/\tau_i) \tag{4}$$

*4,4′-[10,20-Bis(2,4,6-trimethylphenyl)-21*H*,23*H*-porphine-5,15-diyl]bis[benzoic Acid] Dimethyl Ester* **3** was prepared by the method of *Lindsey* and co-workers [53]. UV/VIS (CH_2Cl_2): 418, 516, 550, 592, 650. ^{1}H-NMR (300 MHz, $CDCl_3$): −2.63 (*s*, 2 NH); 1.83 (*s*, 12 H, Me−Ar); 2.62 (*s*, 6 H, Me−Ar); 4.10 (*s*, COOMe); 7.28 (*s*, 4 arom. H); 8.31 (*d*, J = 8, 4 arom. H); 8.43 (*d*, J = 8, 4 arom. H); 8.71 (*AB*, J = 5, 4 H, H−C(β)); 8.74 (*AB*, J = 5, 4 H, H−C(β)). MALDI-TOF-MS: 815 ($C_{54}H_{46}N_4O_4^+$; calc. 815).

*4,4′-[10,20-Bis(2,4,6-trimethylphenyl)-21*H*,23*H*-porphine-5,15-diyl]bis[benzoic Acid] Monomethyl Ester* (**4**). To **3** (1.50 g, 1.84 mmol), CF_3COOH (150 ml) was added and once all the solid had dissolved, conc. HCl soln. (300 ml). The green soln. was warmed to 80° (TLC monitoring). The mixture was cooled as soon as the diacid began to appear (0.5 h). The green mixture was poured into 20% MeOH/$CHCl_3$ (400 ml), the org. phase washed with H_2O until pH 7 was reached, and then evaporated, and the residue chromatographed (silica gel (deactivated with 2% (*w*/*w*) of H_2O), 3–5% MeOH/$CHCl_3$) to separate **4** and residual **3**. The diester **3** was recycled through this process several more times giving rise to a total of 1.10 g of **4** (75%). UV/VIS (CH_2Cl_2): 420, 516, 550, 592, 650. ^{1}H-NMR (300 MHz, $CDCl_3$): −2.62 (*s*, 2 NH); 1.85 (*s*, 12 H, Me−Ar); 2.64 (*s*, 6 H, Me−Ar); 4.11 (*s*, COOMe); 7.29 (*s*, 4 arom. H); 8.32 (*d*, J = 8, 2 arom. H); 8.38 (*d*, J = 8, 2 arom. H); 8.44 (*d*, J = 8, 2 arom. H); 8.54 (*d*, J = 8, 2 arom. H); 8.71–8.79 (*m*, 8 H, H−C(β)). MALDI-TOF-MS: 801 ($C_{53}H_{44}N_4O_4^+$; calc. 801).

*4-[15-(4-Formylphenyl)-10,20-bis(2,4,6-trimethylphenyl)-21*H*-23*H*-porphin-5-yl]benzoic Acid Methyl Ester* (**5**). To a soln. of **4** (400 mg, 0.499 mmol) in THF (60 ml) at 0°, $LiAlH_4$ (50 mg) was added in small portions (TLC monitoring). When reduction of the ester was complete (1 h), the reaction was quenched by adding ice and 0.5M aq. citric acid (5 ml). The mixture was poured into 20% MeOH/$CHCl_3$ (400 ml), the org. phase washed

with H_2O several times and evaporated, and the residue suspended in CH_2Cl_2 and treated with excess diazomethane/Et_2O. The mixture was again evaporated, the solid dissolved in CH_2Cl_2 (50 ml), and activated manganese dioxide added in small portions. After 2 h (TLC: oxidation complete), the solid material was removed by filtration through *Celite*. The filtrate was evaporated and the purple residue chromatographed (silica gel, 5% AcOEt/toluene): 304 mg of **5** (76%). UV/VIS (CH_2Cl_2): 420, 516, 552, 592, 650. ^{1}H-NMR (300 MHz, $CDCl_3$): −2.62 (*s*, 2 NH); 1.83 (*s*, 12 H, Me−Ar); 2.62 (*s*, 6 H, Me−Ar); 4.10 (*s*, COOMe); 7.28 (*s*, 4 arom. H); 8.27 (*d*, *J* = 8, 2 arom. H); 8.30 (*d*, *J* = 8, 2 arom. H); 8.40 (*d*, *J* = 8, 2 arom. H); 8.43 (*d*, *J* = 8, 2 arom. H); 8.70–8.75 (*m*, 8 H, H−C(*β*)); 10.37 (*s*, CHO). MALDI-TOF-MS: 785 ($C_{53}H_{44}N_4O_3^+$; calc. 785).

*4-[15-(4-Formylphenyl)-10,20-bis(2,4,6-trimethylphenyl)-21*H,*23*H*-porphin-5-yl]benzoic Acid* (**6**). A mixture of **5** (400 mg, 0.510 mmol), THF (200 ml) MeOH (80 ml), and 10% aq. KOH soln. (30 ml) was warmed to 40° and stirred for 6 h (TLC monitoring). The mixture was poured into 20% MeOH/$CHCl_3$ and shaken with 1M citric acid (200 ml), and then with H_2O (3×). The org. phase was evaporated: 382 mg (97%) of **6**. UV/VIS (CH_2Cl_2): 420, 516, 552, 592, 650. ^{1}H-NMR (300 MHz, $CDCl_3$): −2.62 (*s*, 2 NH); 1.85 (*s*, 12 H, Me−Ar); 2.64 (*s*, 6 H, Me−Ar); 7.29 (*s*, 4 arom. H); 8.28 (*d*, *J* = 8, 2 arom. H); 8.37 (*d*, *J* = 8, 2 arom. H); 8.42 (*d*, *J* = 8, 2 arom. H); 8.53 (*d*, *J* = 8, 2 arom. H); 8.74–8.78 (*m*, 8 H, H−C(*β*)); 10.39 (*s*, CHO). MALDI-TOF-MS: 771 ($C_{52}H_{42}N_4O_3^+$; calc. 771).

*4-[15-(4-Formylphenyl)-10,20-bis(2,4,6-trimethylphenyl)-21*H,*23*H*-porphin-5-yl]benzoic Acid 3,5-Dimethylbenzyl Ester* (**7**). A soln. of **6** (350 mg, 0.454 mmol) in CH_2Cl_2 (200 ml) was treated with MeOH (100 ml), saturated with $Zn(OAc)_2$ for 3 h. After washing the mixture with H_2O, the solvent was evaporated and the residue dried (UV/VIS (CH_2Cl_2): 420, 520, 558). This material was dissolved in DMF (30 ml), and Li_2CO_3 (40 mg, 0.55 mmol) and 3,5-dimethylbenzyl bromide (0.13 g, 0.64 mmol) were added. The mixture was stirred at r.t. under N_2 for 20 h. As the reaction was incomplete (TLC), a further portion of 3,5-dimethylbenzyl bromide (0.13 g) was added, and a final portion (0.13 g) was added after 30 h. After a total of 48 h, the mixture was poured into Et_2O (200 ml) and washed with H_2O (4×). The solvent was evaporated and the residue dissolved in CH_2Cl_2 (200 ml) containing CF_3COOH (5 ml). After 15 min, the acid was neutralized with sat. $NaHCO_3$ soln. The org. layer was dried (Na_2SO_4) an evaporated and the residue chromatographed (silica gel, 0.5% AcOEt/toluene): 342 mg (85%) of **7**. UV/VIS (CH_2Cl_2): 420, 516, 552, 592, 650. ^{1}H-NMR (300 MHz, $CDCl_3$): −2.62 (*s*, 2 NH); 1.83 (*s*, 12 H, Me−Ar); 2.40 (*s*, 6 H, Me−Ar); 2.62 (*s*, 6 H, Me−Ar); 5.48 (*s*, ArC*H*$_2$); 7.04 (*s*, 1 arom. H); 7.21 (*s*, 2 arom. H); 7.28 (*s*, 4 arom. H); 8.25–8.31 (*m*, 4 arom. H); 8.4 (*d*, *J* = 8, 2 arom. H); 8.46 (*d*, *J* = 8, 2 arom. H); 8.73 (*m*, 8 H, H−C(*β*)); 10.38 (*s*, CHO). MALDI-TOF-MS: 889 ($C_{61}H_{52}N_4O_3^+$; calc. 889).

*4-[15-[4-(1′,5′-Dihydro-1′-methyl-2′*H*-[5,6]fullereno-C$_{60}$-I$_h$-[1,9-c]pyrrol-2′-yl)phenyl]-10,20-bis(2,4,6-trimethylphenyl)-21*H,*23*H*-porphin-5-yl]benzoic Acid 3,5-Dimethylbenzyl Ester* (**8**). A mixture of **7** (200 mg, 0.220 mmol), C_{60} (320 mg, 0.450 mmol), sarcosine (= *N*-methylglycine) (200 mg, 2.25 mmol), and toluene (400 ml) was warmed to reflux under N_2 for 25 h. After cooling, the mixture was evaporated, the residue redissolved in 30% CS_2/toluene, the soln. filtered, and the filtrate applied to a column (silica gel, 0.2% AcOEt/toluene): 290 mg (79%) of **8**. UV/VIS (CH_2Cl_2): 418, 516, 552, 592, 648, 712. ^{1}H-NMR (300 MHz, $CDCl_3$): −2.62 (*s*, 2 NH); 1.80 (*s*, 6 H, Me−Ar); 1.82 (*s*, 6 H, Me−Ar); 2.39 (*s*, 6 H, Me−Ar); 2.61 (*s*, 6 H, Me−Ar); 3.11 (*s*, Me−N); 4.42 (*d*, *J* = 9, 1 pyr. H); 5.10 (*d*, *J* = 9, 1 pyr. H); 5.27 (*s*, 1 pyr. H); 7.04 (*s*, 1 arom. H); 7.20 (*s*, 2 arom. H); 7.25 (*s*, 4 arom. H); 8.20 (br. *s*, 2 arom. H); 8.26–8.30 (*m*, 4 arom. H); 8.45 (*d*, *J* = 8, 2 arom. H); 8.67–8.72 (*m*, 8 H, H−C(*β*)). MALDI-TOF-MS: 1637 ($C_{123}H_{57}N_5O_2^+$; calc. 1637).

*4-[15-[4-(1′,5′-Dihydro-1′-methyl-2′*H*-[5,6]fullereno-C$_{60}$-I$_h$-[1,9-c]pyrrol-2′-yl)phenyl]-10,20-bis(2,4,6-trimethylphenyl)-21*H,*23*H*-porphin-5-yl]benzoic Acid* (**9**). To a soln. of **8** (200 mg, 0.122 mmol) in CH_2Cl_2 (100 ml) at −78°, 1M BBr_3 in CH_2Cl_2 (5 ml) was added dropwise, and the now green soln. was stirred at −78° for 10 min, and then at r.t. for 2 h (TLC: no **8** left, presence of a polar material). The mixture was diluted with 10% MeOH/CH_2Cl_2 (200 ml) and washed with H_2O (3×). The org. phase was evaporated and the residue chromatographed (silica gel (deactivated with 2% H_2O (*w*/*w*)), 5% MeOH/$CHCl_3$): 168 mg (91%) of **9**. UV/VIS (CH_2Cl_2): 420, 516, 552, 592, 650, 710. MALDI-TOF-MS: 1519 ($C_{114}H_{47}N_5O_2^+$; calc. 1519).

*4-[15-[4-(1′,5′-Dihydro-1′-methyl-2′*H*-[5,6]fullereno-C$_{60}$-I$_h$-[1,9-c]pyrrol-2′-yl)phenyl]-10,20-bis(2,4,6-trimethylphenyl)-21*H,*23*H*-porphin-5-yl]benzoic Acid [2-(1,3-Dithiol-2-ylidene)-1,3-dithiol-4-yl]methyl Ester* (**1a**). To **9** (100 mg, 0.061 mmol), CH_2Cl_2 (7 ml), and *N*-methylmorpholine (10 µl, 0.089 mmol) at 0°, 2-chloro-4,6-dimethoxy-1,3,5-triazine (13 mg, 0.072 mmol) was added. The mixture was stirred at 0° for 10 min, then at r.t. for 4 h (TLC: no **9** left, presence of a less-polar material). Subsequently, tetrathiafulvalene-4-methanol [54] (13 mg, 0.056 mmol) and *N*,*N*-dimethylpyridin-4-amine (14 mg, 0.11 mmol) were added. After 1 h, the mixture was diluted with CS_2 (2 ml) and then chromatographed (silica gel, CH_2Cl_2/hexanes/CS_2 6 : 2 : 1): 91 mg (80%) of **1a**. UV/VIS (CH_2Cl_2) 424, 516, 550, 592, 648, 704. ^{1}H-NMR (500 MHz, $CDCl_3$): −2.71 (*s*, 2 NH); 1.78 (*s*, 6 H, Me−Ar); 1.80 (*s*, 6 H, Me−Ar); 2.58 (*s*, 6 H, Me−Ar); 3.11 (*s*, Me−N); 4.42 (*d*, *J* = 9, 1 pyr. H); 5.09 (*d*, *J* = 9,

1 pyr. H); 5.18 (*s*, CH_2O); 5.26 (*s*, 1 pyr. H); 6.27 (*s*, 2 H, =CH); 6.45 (*s*, 1 H, =CH); 7.21 (*s*, 4 arom. H); 8.17 (br. *s*, 2 arom. H); 8.22 (*d*, *J* = 7, 2 arom. H); 8.26 (*d*, *J* = 8, 2 arom. H); 8.39 (*d*, *J* = 8, 2 arom. H); 8.58 (br. *s*, 4 H, H−C(*β*)); 8.60 (*d*, *J* = 5, 4 H, H−C(*β*)); 8.67 (*d*, *J* = 5, 4 H, H−C(*β*)). FAB-MS: 1734.3020 ($[M+H]^+$, $C_{121}H_{51}N_5O_2S_4^+$; calc. 1733.2962).

*{[2-(1,3-Dithiol-2-ylidene)-1,3-dithiol-4-yl]methyl 4-[15-[4-(1′,5′-Dihydro-1′-methyl-2′*H*-[5,6]fullereno-C_{60}-I_h-[1,9-c]pyrrol-2′-yl)phenyl]-10,20-bis(2,4,6-trimethylphenyl-21*H*,23*H*-porphin-5-yl-κN^{21},κN^{22},κN^{23},κN^{24}]benzoato(2−)}zinc* (**1b**). As needed, a small portion of **1a** in CH_2Cl_2 and an excess of $Zn(OAc)_2$ were stirred, and **1b** was isolated by TLC (silica gel).

*4,4′-[10,20-Bis(2,4,6-trimethylphenyl)-21*H*,23*H*-porphine-5,15-diyl]bis[benzoic Acid] [2-(1,3-Dithiol-2-ylidene)-1,3-dithiol-4-yl]methyl Methyl Ester* (**2a**). To a soln. of **4** (60 mg, 0.075 mmol), CH_2Cl_2 (6 ml), and *N*-methylmorpholine (12 µl, 0.11 mmol) at 0°, 2-chloro-4,6-dimethoxy-1,3,5-triazine (16 mg, 0.089 mmol) was added. Stirring was continued for 15 min at 0° and then at r.t. for 3 h. Portions of tetrathiafulvalene-4-methanol (16 mg, 0.068 mmol) and *N*,*N*-dimethyl pyridin-4-amine (17 mg, 0.14 mmol) were added, and stirring was continued for 1 h. The mixture was diluted with hexanes (2 ml) and the soln. chromatographed (silica gel, 25% hexanes/CH_2Cl_2): 61 mg (80%) of **2a**. UV/VIS (CH_2Cl_2): 420, 516, 550, 592, 648. ^{1}H-NMR (300 MHz, $CDCl_3$): −2.64 (*s*, 2 NH); 1.84 (*s*, 12 H, Me−Ar); 2.62 (*s*, 6 H, Me−Ar); 4.11 (*s*, COOMe); 5.24 (*s*, CH_2O); 6.32 (*s*, 2 H, =CH); 6.53 (*s*, 1 H, =CH); 7.28 (*s*, 4 arom. H); 8.30 (*d*, *J* = 3, 2 arom. H); 8.33 (*d*, *J* = 3, 2 arom. H); 8.42 (*d*, *J* = 3, 2 arom. H); 8.45 (*d*, *J* = 3, 2 arom. H); 8.72 (*AB*, *J* = 5, 4 H, H−C(*β*)); 8.74 (*AB*, *J* = 5, 4 H, H−C(*β*)). MALDI-TOF-MS: 1017 ($C_{60}H_{48}N_4O_4S_4^+$; calc. 1017).

*{[2-(1,3-Dithiol-2-ylidene)-1,3-dithiol-4-yl]methyl Methyl 4,4′-[10,20-Bis(2,4,6-trimethylphenyl)-21*H*,23*H*-porphine-5,15-diyl-κN^{21},κN^{22},κN^{23},κN^{24}]-bis[benzoate](2−)}zinc* (**2b**). As needed, a small portion of **2a** in CH_2Cl_2 and an excess of $Zn(OAc)_2$ were stirred, and **2b** was isolated by TLC (silica gel).

[2-(1,3-Dithiol-2-ylidene)-1,3-dithiol-4-yl]methyl 4-Methylbenzoate (**10**). A mixture of tetrathiafulvalene-4-methanol (50 mg, 0.12 mmol), CH_2Cl_2 (12 ml), pyridine (52 µl, 0.64 mmol) and 4-methylbenzoyl chloride (56 µl, 0.43 mmol) was stirred at r.t. under N_2 for 1 h, and then diluted with CH_2Cl_2 (60 ml). This soln. was washed with 2M HCl, and then with sat. $NaHCO_3$ soln., dried (Na_2SO_4), and evaporated and the residue chromatographed (silica gel, 33% hexanes/toluene): 73 mg (97%) of **10**. UV/VIS (CH_2Cl_2): 241, 317, 366, 464. ^{1}H-NMR (300 MHz, $CDCl_3$): 2.41 (*s*, 3 H, Me−Ar); 5.04 (*s*, CH_2O); 6.31 (*s*, 2 H, =CH); 6.40 (*s*, 1 H, =CH); 7.25 (*d*, *J* = 8, 2 arom. H); 7.94 (*d*, *J* = 8, 2 arom. H). MALDI-TOF-MS: 352 ($C_{15}H_{12}O_2S_4^+$; calc. 352).

This work was supported by a grant from the *National Science Foundation* (CHE-0078835). FAB-MS Studies were performed by the *Midwest Center for Mass Spectrometry*, with partial support by the *National Science Foundation* (DIR9017262). This is publication 495 from the ASU Center for the Study of Early Events in Photosynthesis.

REFERENCES

[1] D. Gust, T. A. Moore, A. L. Moore, *Acc. Chem. Res.* **2001**, *34*, 40.
[2] D. Gust, T. A. Moore, in 'The Porphyrin Handbook', Ed. K. M. Kadish, K. M. Smith, R. Guilard, Academic Press, New York, 2000, Vol. 8, p. 153.
[3] D. Gust, T. A. Moore, A. L. Moore, *Acc. Chem. Res.* **1993**, *26*, 198.
[4] D. Gust, T. A. Moore, *Adv. Photochem.* **1991**, *16*, 1.
[5] M. R. Wasielewski, *Chem. Rev.* **1992**, *92*, 435.
[6] M. Bixon, J. Fajer, G. Feher, J. H. Freed, D. Gamliel, A. J. Hoff, H. Levanon, K. Möbius, R. Nechushtai, J. R. Norris, A. Scherz, J. L. Sessler, D. Stehlik, *Isr. J. Chem.* **1992**, *32*, 449.
[7] T. Asahi, M. Ohkouchi, R. Matsusaka, N. Mataga, R. P. Zhang, A. Osuka, K. Maruyama, *J. Am. Chem. Soc.* **1993**, *115*, 5665.
[8] J. S. Connolly, J. R. Bolton, in 'Photoinduced Electron Transfer, Part D', Ed. M. A. Fox, M. Chanon, Elsevier, Amsterdam, 1988, p. 303.
[9] Y. Sakata, H. Imahori, H. Tsue, S. Higashida, T. Akiyama, E. Yoshizawa, M. Aoki, K. Yamada, K. Hagiwara, S. Taniguchi, T. Okada, *Pure Appl. Chem.* **1997**, *69*, 1951.
[10] H. Imahori, Y. Sakata, *Adv. Mater.* **1997**, *9*, 537.
[11] D. Kuciauskas, P. A. Liddell, S. Lin, T. E. Johnson, S. J. Weghorn, J. S. Lindsey, A. L. Moore, T. A. Moore, D. Gust, *J. Am. Chem. Soc.* **1999**, *121*, 8604.
[12] G. Steinberg-Yfrach, P. A. Liddell, S.-C. Hung, A. L. Moore, D. Gust, T. A. Moore, *Nature (London)* **1997**, *385*, 239.

[13] G. Steinberg-Yfrach, J.-L. Rigaud, E. N. Durantini, A. L. Moore, D. Gust, T. A. Moore, *Nature (London)* **1998**, *392*, 479.
[14] J. L. Bahr, D. Kuciauskas, P. A. Liddell, A. L. Moore, T. A. Moore, D. Gust, *J. Photochem. Photobiol*. **2000**, *72*, 598.
[15] D. Carbonera, M. Di Valentin, C. Corvaja, G. Agostini, G. Giacometti, P. A. Liddell, D. Kuciauskas, A. L. Moore, T. A. Moore, D. Gust, *J. Am. Chem. Soc*. **1998**, *120*, 4398.
[16] D. Gust, T. A. Moore, A. L. Moore, P. A. Liddell, D. Kuciauskas, J. P. Sumida, B. Nash, D. Nguyen, in 'Recent Advances in the Chemistry and Physics of Fullerenes and Related Materials', Ed. K. M. Kadish, A. W. Rutherford, The Electrochemical Society, Pennington, NJ, 1997, Vol. 4. p. 9.
[17] D. Gust, T. A. Moore, A. L. Moore, D. Kuciauskas, P. A. Liddell, B. D. Halbert, *J. Photochem. Photobiol. B* **1998**, *43*, 209.
[18] D. Kuciauskas, P. A. Liddell, T. A. Moore, A. L. Moore, D. Gust, in 'Recent Advances in the Chemistry and Physics of Fullerenes and Related Materials', Ed. K. M. Kadish, R. S. Ruoff, The Electrochemical Society, Pennington, N. J., 1998, Vol. 6, p. 242.
[19] D. Kuciauskas, P. A. Liddell, A. L. Moore, T. A. Moore, D. Gust, *J. Am. Chem. Soc*. **1998**, *120*, 10880.
[20] D. Kuciauskas, P. A. Liddell, S. Lin, S. Stone, A. L. Moore, T. A. Moore, D. Gust, *J. Phys. Chem. B* **2000**, *104*, 4307.
[21] P. A. Liddell, D. Kuciauskas, J. P. Sumida, B. Nash, D. Nguyen, A. L. Moore, T. A. Moore, D. Gust, *J. Am. Chem. Soc*. **1997**, *119*, 1400.
[22] P. R. Ashton, V. Balzani, J. Becher, A. Credi, M. C. T. Fyfe, G. Mattersteig, S. Menzer, M. B. Nielsen, F. M. Raymo, J. F. Stoddart, M. Venturi, D. J. Williams, *J. Am. Chem. Soc*. **1999**, *121*, 3951.
[23] M. A. Herranz, B. Illescas, N. Martin, C. P. Luo, D. M. Guldi, *J. Org. Chem*. **2000**, *65*, 5728.
[24] N. Martin, L. Sanchez, M. A. Herranz, D. M. Guldi, *J. Phys. Chem. A* **2000**, *104*, 4648.
[25] M. A. Herranz, N. Martin, L. Sanchez, C. Seoane, D. M. Guldi, *J. Organomet. Chem*. **2000**, *599*, 2.
[26] M. Prato, M. Maggini, C. Giacometti, G. Scorrano, G. Sandona, G. Farnia, *Tetrahedron* **1996**, *52*, 5221.
[27] N. Martin, L. Sanchez, C. Seoane, R. Andreu, J. Garin, J. Orduna, *Tetrahedron Lett*. **1996**, *37*, 5979.
[28] N. Martin, I. Perez, L. Sanchez, C. Seoane, *J. Org. Chem.* **1997**, *62*, 5690.
[29] C. Boulle, J. M. Rabreau, P. Hudhomme, M. Cariou, M. Jubault, A. Gorgues, J. Orduna, J. Garin, *Tetrahedron Lett*. **1997**, *38*, 3909.
[30] M. R. Bryce, *Adv. Mater*. **1999**, *11*, 11.
[31] J. Llacay, J. Veciana, J. Vidal-Gancedo, J. L. Bourdelande, R. Gonzalez-Moreno, C. Rovira, *J. Org. Chem*. **1998**, *63*, 5201.
[32] J. Llacay, M. Mas, E. Molins, J. Veciana, D. Powell, C. Rovira, *Chem. Commun*. **1997**, 659.
[33] M. R. Bryce, *J. Mater. Chem.* **2000**, *10*, 589.
[34] D. M. Guldi, S. Gonzalez, N. Martin, A. Anton, J. Garin, J. Orduna, *J. Org. Chem*. **2000**, *65*, 1978.
[35] M. Maggini, G. Scorrano, M. Prato, *J. Am. Chem. Soc*. **1993**, *115*, 9798.
[36] G. Kodis, P. A. Liddell, L. de la Garza, P. C. Clausen, J. S. Lindsey, A. L. Moore, T. A. Moore, D. Gust, personal communication.
[37] D. C. Green, *J. Org. Chem*. **1979**, *44*, 1476.
[38] D. Kuciauskas, S. Lin, G. R. Seely, A. L. Moore, T. A. Moore, D. Gust, T. Drovetskaya, C. A. Reed, P. D. W. Boyd, *J. Phys. Chem*. **1996**, *100*, 15, 926.
[39] G. H. Golub, C. Reinsch, *Numer. Math*. **1970**, *14*, 403.
[40] E. R. Henry, J. Hofrichter, in 'Methods in Enzymology', Ed. B. Ludwig, Academic Press, San Diego, 1992, Vol. 210, p. 219.
[41] R. A. Marcus, *J. Chem. Phys.* **1956**, *24*, 966.
[42] R. A. Marcus, *J. Chem. Phys.* **1965**, *43*, 2654.
[43] D. M. Guldi, K.-D. Asmus, *J. Am. Chem. Soc*. **1997**, *119*, 5744.
[44] H. Imahori, K. Hagiwara, M. Aoki, T. Akiyama, S. Taniguchi, T. Okada, M. Shirakawa, Y. Sakata, *J. Am. Chem. Soc*. **1996**, *118*, 11771.
[45] H. Imahori, K. Hagiwara, T. Akiyama, M. Aoki, S. Taniguchi, T. Okada, M. Shirakawa, Y. Sakata, *Chem. Phys. Lett*. **1996**, *263*, 545.
[46] S. Larsson, A. Klimkans, L. Rodriguez-Monge, G. Duskesas, *J. Mol. Struct.* **1998**, *425*, 155.
[47] D. Gust, T. A. Moore, L. R. Makings, P. A. Liddell, G. A. Nemeth, A. L. Moore, *J. Am. Chem. Soc*. **1986**, *108*, 8028.
[48] M. Ohkouchi, A. Takahashi, N. Mataga, T. Okada, A. Osuka, H. Yamada, K. Maruyama, *J. Am. Chem. Soc*. **1993**, *115*, 12137.

[49] A. Osuka, H. Yamada, T. Shinoda, K. Nozaki, O. Ohno, *Chem. Phys. Lett*. **1995**, *238*, 37.
[50] D. Gust, T. A. Moore, D. K. Luttrull, G. R. Seely, E. Bittersmann, R. V. Bensasson, M. Rougée, E. J. Land, F. C. de Schryver, M. Van der Auweraer, *Photochem. Photobiol*. **1990**, *51*, 419.
[51] F. S. Davis, G. A. Nemeth, D. M. Anjo, L. R. Makings, D. Gust, T. A. Moore, *Rev. Sci. Instrum*. **1987**, *58*, 1629.
[52] A. Freiberg, K. Timpmann, S. Lin, N. W. Woodbury, *J. Phys. Chem. B* **1998**, *102*, 10974.
[53] C.-H. Lee, J. S. Lindsey, *Tetrahedron* **1994**, *50*, 11427.
[54] J. Garin, J. Orduna, S. Uriel, A. J. Moore, M. R. Bryce, S. Wegener, D. S. Yufit, J. A. K. Howard, *Synthesis* **1994**, 493.

Received May 31, 2001